JOURNAL OF AIRCRAFT
Vol. 54, No. 4, July–August 2017

Genetic Algorithm-Based Model Order Reduction of Aeroservoelastic Systems with Consistent States

Jin Zhu,* Yi Wang,† and Kapil Pant‡
CFD Research Corporation, Huntsville, Alabama 35806
and
Peter M. Suh§ and Martin J. Brenner¶
NASA Armstrong Flight Research Center, Edwards, California 93523

DOI: 10.2514/1.C034129

This paper presents a model order reduction framework to construct linear parameter-varying reduced-order models of flexible aircraft for aeroservoelasticity analysis and control synthesis in broad two-dimensional flight parameter space. Genetic algorithms are used to automatically determine physical states for reduction and to generate reduced-order models at grid points within parameter space while minimizing the trial-and-error process. In addition, balanced truncation for unstable systems is used in conjunction with the congruence transformation technique to achieve locally optimal realization and "weak" fulfillment of state consistency across the entire parameter space. Therefore, aeroservoelasticity reduced-order models at any flight condition can be obtained simply through model interpolation. The methodology is applied to the pitch-plant model of the X-56A Multi-Use Technology Testbed currently being tested at NASA Armstrong Flight Research Center for flutter suppression and gust load alleviation. The present studies indicate that the reduced-order model with more than 12× reduction in the number of states relative to the original model is able to accurately predict system response among all input–output channels. The genetic-algorithm-guided approach exceeds manual and empirical state selection in terms of efficiency and accuracy. The interpolated aeroservoelasticity reduced-order models exhibit smooth pole transition and continuously varying gains along a set of prescribed flight conditions, which verifies consistent state representation obtained by congruence transformation. The present model order reduction framework can be used by control engineers for robust aeroservoelasticity controller synthesis and novel vehicle design.

Nomenclature

A	=	state matrix
B	=	input matrix
C	=	output state matrix
D	=	input transition
f_l	=	individual fitness value
i	=	index for grid points in the parameter space
J_l	=	individual objective function value
M	=	matrices in state-space model
$\tilde{P}$	=	generalized controllability gramian
$\tilde{Q}$	=	generalized observability gramian
R	=	common subspace for reprojection
S	=	singular value matrix
u	=	input signals
$\tilde{V}$	=	transformation matrix in balanced realization
$\tilde{W}$	=	transformation matrix in balanced realization
y	=	response measurements
x	=	system state
Γ	=	transformation matrix for consistent state representation
ρ	=	vector of measurable parameters

Subscript

r	=	reduced system states and matrices without consistency

Superscript

*	=	reduced system states and matrices with consistence

I. Introduction

WITH the fast-paced technological advances in this new era of science, modern aerospace designs are able to incorporate new flexible structures and lighter materials to achieve enhanced maneuverability, endurance, and performance. As a result, they are also more susceptible to issues such as complex dynamics and interactions between the controller and the aerodynamic and structural systems, which may lead to adverse events such as flutter, limit-cycle oscillation, and gust loading. To design a modern flexible aircraft that can attain a safe and acceptable flight envelope, detailed modeling and high-fidelity simulations of aeroservoelastic (ASE) systems must be performed before flight tests to investigate the source of potential aeroelastic (AE) failures. Although full-order models that couple the nonlinear aerodynamics with structural models are capable of accurate prediction of underlying AE phenomena and onset, their prohibitive computational cost, low speed, nonlinear nature, and difficulty to deploy controllers with high-state-order models render them impractical for integration in the design environment involving concurrent ASE analysis and control synthesis and design.

To combat these challenges, various model order reduction (MOR) techniques have been developed in the context of linear parameter-varying (LPV) formulation. In LPV, the fully coupled nonlinear aircraft model is represented as an ensemble of linearized models at the grid points within the parameter space, and the model parameters vary across the flight envelope. Models at any location within the domain can be obtained by interpolating those at the grid points. MOR aims to reduce the full-order LPV ASE model into a reduced state-space form while retaining the dominant dynamics of the system in the target frequency range where AE may be involved. MOR can be classified into nontransformation (e.g., truncation and residualization) and transformation-based techniques, such as modal reduction, balanced truncation, Krylov subspace

Received 15 July 2016; revision received 23 September 2016; accepted for publication 17 October 2016; published online 13 January 2017.

*Associate Engineer.
†Director; yi.wang@cfdrc.com. Member AIAA (Corresponding Author).
‡Vice President.
§Aerospace Engineer, Aerostructures Branch. Member AIAA.
¶Aerospace Engineer, Aerostructures Branch. Senior Member AIAA.

projection, hybrid singular value decomposition (SVD)–Krylov approaches [1], etc. Although yielding reduced-order models (ROMs) with consistent states amenable to direct model interpolation, the former typically is a trial-and-error and/or empirical process that manually examines and selects unimportant states to eliminate from the original systems in an iterative manner. On the other hand, for the transformation-based MOR techniques, although more efficient and accurate given tight state budgets, the optimal transformation is flight-parameter-dependent, leading to different state meanings of the ROMs at various locations in the flight envelope, which leads to state inconsistency of the LPV system and makes facile interpolation impossible. To form LPV ROMs encompassing the entire parameter space, several techniques have been proposed for consistent state representation and ROM interpolation. Hjartarson et al. [2] proposed to apply the transformation matrix obtained by balanced truncation at a single flight condition to the LPV model sets within the entire flight envelope. Although maintaining state consistency, the approach is suboptimal because balancing transformation by nature changes with flight parameter. Moreno et al. [3] used a contractive right coprime factorization approach to attain consistent controllability and observability gramians throughout the flight envelope, which can be balanced to achieve state consistency. This approach suffers from several inherent limitations, such as challenges in use over broad and high-dimensional parameter space as well as numerical issues associated with large state numbers. Panzer et al. [4] proposed two methods, respectively, based on reprojection onto a common subspace and optimization-based matrix matching to achieve identical state meanings among local models for interpolation. The former was employed for interpolating LPV ROMs of industrial flexible aircraft [5]. The common subspace in [4] is obtained by SVD of the ensemble of transformation matrices at various parameters and, hence, is ill-suited for use in broad flight envelope including dramatically varying parameters. Poussot-Vassal and Demourant [6] compared several MOR techniques and their application to aircraft systems, including balanced truncation, iterative tangential interpolation algorithm, and iterative SVD-tangential interpolation algorithms along with a modal form-based coordinate transformation to achieve state consistency. Theis et al. [7] developed a new modal matching technique, which casts ROMs into a modewise canonical form and matches modes with similar dynamic properties at neighboring grid points to minimize state inconsistency.

In spite of seminal works in MOR of ASE systems, there still exist several challenges to be addressed to propagate the application of these techniques. For example, automated selection of physical states within various aircraft components for reduction without trial-and-error or prior knowledge of the model is needed to render the approach directly applicable to a completely new aircraft model. In order to obtain consistent state representation among local ROMs, capabilities need to be developed to tackle more complex scenarios, such as inherently unstable ASE systems in two-dimensional (2-D) or even high-dimensional flight parameter space involving pole conversion (i.e., real poles change into conjugate pairs or vice versa).

In this context, this paper presents the development of LPV ASE reduced-order models (ROMs) of flexible aircraft based on a combination of automated model reduction, consistent state representation, and model interpolation approaches. The X-56A MUTT vehicle with flexible wings currently being tested at NASA Armstrong Flight Research Center for flutter suppression and gust load alleviation was used for analysis, verification, and demonstration. In the MOR, the truncation and residualization methods were first applied to the states of sensors, actuators, aerodynamic lags, rigid bodies, and elastic structures of the full-order X-56A Multi-Use Technology Testbed (MUTT) ASE model on the grid points in the flight parameter space. In contrast to previous efforts [2,3,8], for the first time, a process based on genetic algorithm (GA) and globally averaged objective function was developed for automated selection of unimportant states in the aerodynamic lag and the elastic modes to truncate/residualize, which not only eliminates the manual, trial-and-error process for state screening but also improves MOR accuracy and performance given state budgets. The balanced truncation for unstable systems was also used to further reduce states with minor contribution to the input/output energy of the system in the local ROMs. Finally, the method of congruence transformation was exploited to remedy the issue of inconsistent state representation among local ROMs caused by flight-parameter-dependent transformation (caused by balanced truncation). Different from previous approaches of modal matching [7], modal canonical form [6], and reprojection onto a common subspace [4,5,8], the congruence transformation harnesses basis information in the transformation matrices and allows weak fulfillment of the modal assurance criterion (MAC), rendering ROM interpolation possible to construct a unified LPV ROM feasible across a broader flight envelope.

II. Linear Parameter-Varying Aeroservoelastic Models of Aircraft

Linear parameter-varying (LPV) models are state-space models whose mathematical descriptions are functions of time-varying parameters, i.e.,

$$\begin{bmatrix} \dot{x} \\ y \end{bmatrix} = \begin{bmatrix} A(\rho) & B(\rho) \\ C(\rho) & D(\rho) \end{bmatrix} \begin{bmatrix} x(t) \\ u(t) \end{bmatrix} \tag{1}$$

where $A(\rho)$ is the state matrix; $B(\rho)$ is the input matrix; $C(\rho)$ is the output state matrix; $D(\rho)$ is the input transition matrix; $\rho \in \mathfrak{R}^{\text{np}}$ is a vector of measurable parameters, e.g., fuel weights and knots equivalent airspeed (KEAS) in the present work; and $u \in \mathfrak{R}^{\text{nu}}$ and $y \in \mathfrak{R}^{\text{ny}}$ are, respectively, the vector of the control inputs and measurement outputs. There are several methods to represent parameter dependence in the preceding LPV models, such as linear fractional transformation, polytopic dependence of the state matrix on the parameters, linearization on a gridded domain, etc. This paper targets the MOR of LPV models based on the gridded domain, in which the nonlinear dynamics in the ASE system of the flexible aircraft is linearized around various flight conditions, also termed grid points or parameter locations hereafter. The resulting set of original, full-order linear time-invariant (LTI) state-space models at grid points are then reduced using our MOR techniques, followed by constructing LPV-ROM via model interpolation that is applicable to the entire flight parameter space. Eventually, the ROM can be used for real-time ASE simulation, system-level analysis, and controller synthesis.

III. Model Order Reduction for Linear Parameter-Varying Aeroservoelastic Models of Flexible Aircraft

Figure 1 illustrates our MOR methodology for LPV ASE models of flexible aircraft. A prerequisite of the approach is to first have a set of full-order LTI state-space models describing coupled ASE behavior at grid points in the flight parameter space. The full model can be generated from relevant modeling tools (see Sec. IV). The entire MOR process includes two key steps.

1) Local MOR (the middle column in Fig. 1): the original, full-order LTI model set is first reduced and transformed onto a low-dimension subspace yielding a set of local ROMs. Several techniques can be used, including truncation and residualization, and transformation and truncation (e.g., modal reduction and balanced realization and truncation, Krylov methods, and their combinations). Because the transformation/projection matrices used depend on the location of the grid points, measures need to be taken to ensure that all ROMs are cast in a consistent state representation (or coordinates) before model interpolation.

2) ROM interpolation: the ROM at any location within the flight envelope is then obtained by interpolating the system matrices of the local ROM set obtained in the previous step.

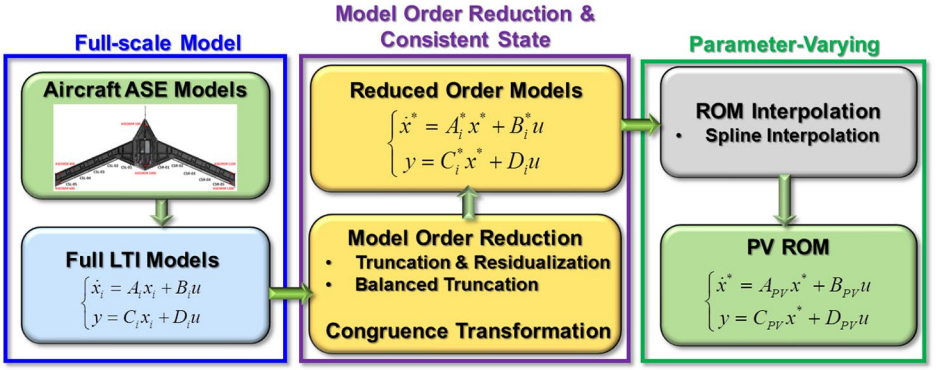

Fig. 1 Organization of LPV MOR framework.

Equation (2) summarizes the MOR process:

$$\begin{bmatrix} \dot{x} \\ y \end{bmatrix} = \begin{bmatrix} A_i & B_i \\ C_i & D_i \end{bmatrix} \begin{bmatrix} x(t) \\ u(t) \end{bmatrix} \xrightarrow[\text{Represenation}]{\text{MOR}} \begin{bmatrix} \dot{x}^* \\ y \end{bmatrix}$$
$$= \begin{bmatrix} A_i^* & B_i^* \\ C_i^* & D_i \end{bmatrix} \begin{bmatrix} x^* \\ u(t) \end{bmatrix} \xrightarrow[\text{Interpolation}]{\text{LPV ROM}} \begin{bmatrix} \dot{x}^* \\ y \end{bmatrix}$$
$$= \begin{bmatrix} A_{\text{PV}}(\rho) & B_{\text{PV}}(\rho) \\ C_{\text{PV}}(\rho) & D_{\text{PV}}(\rho) \end{bmatrix} \begin{bmatrix} x^* \\ u(t) \end{bmatrix} \tag{2}$$

where i denotes the ith grid point in the parameter space; the asterisk $*$ denotes the reduced system with consistent state representation; and the subscript PV denotes the parameter-varying ROM encompassing the entire parameter space and obtained via model interpolation. Note that, because of the flight dynamics of X-56A and consistent transformation matrices following congruence transformation (later), the parameter rate $\dot{\rho}$ is assumed to be negligible.

Two techniques are used primarily in our framework for local MOR, namely, truncation and residualization and balanced truncation for unstable systems, as described in Secs. III.A and III.C, respectively. The truncation and residualization will be first used to remove unimportant states in common among all grid points without altering state consistency and to eliminate the states around the imaginary axis to further improve MOR performance downstream. It is then followed by balanced truncation to further refine the model from the input/output channel energy perspective. There are three facets that distinguish the current effort from the previous.

1) Rather than relying on heuristics and trial-and-error, a genetic algorithm (GA)-based procedure is developed to "intelligently" determine which states to retain (or remove) in the aforementioned truncation and residualization.

2) In contrast to previous research [7,8], including ours, the modal reduction approach based on the real and ordered eigenstructure decomposition was not used herein. This is because the modal frequency varies significantly across the broad 2-D flight parameter space, and the full models at various grid points may have a different number of complex and real poles. It was found in our investigation that the use of modal reduction causes substantial state inconsistence among local ROMs.

3) Instead of using the modal matching [7] or the canonical modal form [6] to achieve consistent state representation, congruence transformation appears more promising in handling LPV models in 2-D parameter space involving the issue of pole conversion (i.e., real poles change into conjugate pairs or vice versa) [7].

A. Truncation and Residualization

MOR by truncation and residualization essentially partitions the state vector x in the model into two components $[x_1 x_2]^T$, where x_1 are the states to keep and x_2 are those to eliminate. Therefore, the system matrices A, B, and C can be partitioned as

$$A = \begin{bmatrix} A_{11} & A_{12} \\ A_{21} & A_{22} \end{bmatrix}, \qquad B = \begin{bmatrix} B_1 \\ B_2 \end{bmatrix}, \qquad C = [C_1 \quad C_2] \tag{3}$$

The ROM is obtained by truncating all the terms associated with x_2. Truncation preserves the ROM accuracy at high frequencies. When the steady-state gain of a system needs to be retained, a residualization procedure is implemented, in which the state derivatives for x_2 are set to zero, leading to a more accurate approximation of the original system at low frequency. The residualized ROM is then given by

$$\begin{bmatrix} \dot{x}_1 \\ y \end{bmatrix} = \begin{bmatrix} (A_{11} - A_{12}A_{22}^{-1}A_{21}) & (B_1 - A_{12}A_{22}^{-1}B_2) \\ (C_1 - C_2A_{22}^{-1}A_{21}) & (D - C_2A_{22}^{-1}B_2) \end{bmatrix} \begin{bmatrix} x_1(t) \\ u(t) \end{bmatrix} \tag{4}$$

B. Genetic-Algorithm-Guided Truncation and Residualization

The preceding truncation and residualization will be employed to reduce states under various categories, such as sensors, actuators, rigid body, aerodynamic lag, elastic states, etc., of the ASE system [2,3,8–10]. The challenge is to determine which states to keep or remove. Previously, this was performed based on the understanding of the vehicle dynamics [3,9], iterative process [2], retention of the states corresponding to leading modes [8], etc., which are mostly empirical. In this paper, a global optimization approach based on the genetic algorithm was developed for automatic state selection and reduction with minimal reliance on the user's experience and trial-and-error process while maintaining dynamics of the original system.

A genetic algorithm (GA) is a stochastic global search method designed to mimic evolution and natural selection. GAs use a multitude of initial potential solutions (often called a population) to sample the entire solution space and then use the process of natural selection to evaluate the population based on the individual fitness levels of its chromosomes (member of the population) to better approximate the optimal solution [11]. This process takes many generations to converge, and at each generation, a new population is created based on the fitness level of the previous generation. As shown in Fig. 2, most GA applications have four key aspects: crossover, mutation, objective function, and fitness function/selection. The process starts with an initial population. A population is a set of binary strings (often called genotypes or chromosomes), each of which is a potential solution to the optimization problem. The chromosomes must be altered in a certain way to approach the optimal solution, which in our case is the most important states to retain. In all stochastics-based algorithms, there is a tradeoff between exploration (sampling the solution space) and exploitation (fixing the solution on the global minimum). In GA, the role of the exploitation falls on the crossover operator and that of the exploration on the mutation operator [11]. The crossover operator is used as an exploitation tool and combines portions of two parent chromosomes that are already "good", with the goal to generate offspring approaching closer to the global minimum. Only using crossover

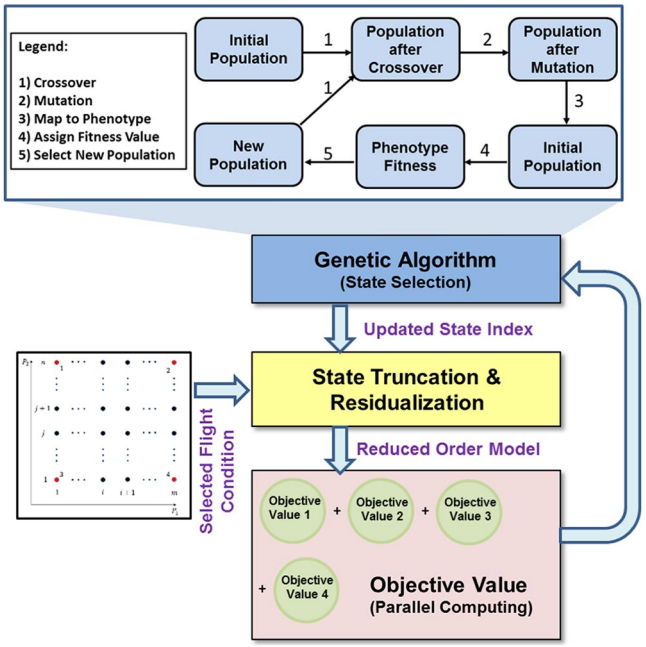

Fig. 2 Schematic of truncation and residualization along with the generic algorithm for automated state selection.

within a GA is prone to be trapped with a local minimum [12,13]. For binary encoding, the mutation operator typically uses bit inversion to accomplish its task. Each gene is altered independently of others, typically with a probability of $1/L$, where L is bounded by the length of the population size and the length of the chromosome. The probability of mutation is usually very low because its main purpose is to maintain diversity within the population and ensure that the solution does not prematurely converge. We also devised a way to decode the binary strings carried by chromosomes into a physical solution. An index of 1 indicates that the state would be kept, and 0 would be removed. For example, consider a system with state vector $x = [x_1\ x_2\ x_3\ x_4\ x_5]^T$ that has the binary representation $[1\quad 1\quad 0\quad 1\quad 0]$, indicating that the reduced system has the configuration $x_r = [x_1\ x_2\ x_4]^T$ with x_3 and x_5 eliminated.

Similar to any optimization problem, one key aspect of GA is the objective/cost function. The goal of MOR is to reduce the number of states in the ASE system while preserving system responses along target input–output channels. Hence, in this paper, the objective function is the difference in the infinity norm H_∞ between the original model and the ROM:

$$J = \|(G(j\omega) - G_r(j\omega))\|_\infty \tag{5}$$

where G and G_r, respectively, represent the dynamic system before and after the truncation and residualization. GA essentially locates the most important states and keeps them in the reduced system to approximate the original one with minimal error. To evaluate the fitness level of the candidate population, a fitness function is defined, which yields high fitness values f_l, whereas the objective function value J is low:

$$f_l = (c/J_l)^n \quad \text{and} \quad P_l = f_l / \sum_{l=1}^{n_g} f_l \tag{6}$$

where c and n are constant weights, l is the lth genome in the population, and n_g is the total number of genome for interrogation in the population. Then, the roulette wheel method is used to select which genomes to move onto the next generation. Specifically, each genome is assigned a probability of survival P_l based on its individual fitness value in the population. It is clear that the higher the fitness value is, the more likely the genome is to survive to the next generation. The flowchart of the GA for state selection is summarized in the top inset of Fig. 2.

Note that, in a gridded LPV system, the optimal states identified by the GA may vary across flight parameters, which, however, is undesired because it causes mismatch in state representation among local ROMs and difficulties for model interpolation downstream. Instead, we use the four most-extreme flight conditions, viz., $[50\quad 100]\text{KEAS} \times [0\quad 80]$ lb as probes or representative grids for the 2-D flight parameter space. Given a budget of the number of states, the GA determined a common set of states that are applied simultaneously to reduce the full model at these four grid points. Correspondingly, the objective function value was taken to be the average of the individual objective function values at these points. Thus, the identified states represent a globally optimal selection among various flight conditions. Moreover, calculating individual objective function values is an independent process for each of the selected flight conditions, and hence, the parfor loop in MATLAB's Parallel Computing Toolbox was used in lieu of the standard for loop to accelerate the GA process that involves many generations to converge to the global state selection. The objective function evaluation is independent from each other, leading to salient linearity in speedup ~4×. Figure 2 summarizes the work flow of the state truncation and residualization in conjunction with the genetic algorithm (GA). The GA starts with a population with initial genomes encoding the state indices for reduction. The objective function values quantifying the difference in infinity norm between the original model and the reduced model are then evaluated and returned to the GA for determining optimal genomes and its encoded state indices for the next iteration/generation. Although only four extreme flight conditions are used as the performance probes in this paper (furthest dots at the four corners in Fig. 2), more parameters at critical regions can be incorporated for preferential local consideration.

C. Balanced Residualization and Truncation for Unstable System

The presence of parameter-dependent unstable states in the ASE model of flexible aircraft causes formidable challenges and complexities for MOR and consistent state representation. The unstable states should be retained in the reduced-order system to perform controller synthesis for stabilization and damping augmentation of the ASE system. Traditionally, a stable/antistable separation is carried out before balanced truncation, and the balancing transformation is only applied to the stable parts, whereas the unstable part remains intact (e.g., functions balreal and balancmr in Matlab). In the present effort, the balanced truncation for unstable

systems based on generalized representation of the gramians proposed by Zhou et al. [14] is employed. The generalized gramian of unstable systems is well-defined when there are no poles on the imaginary axis and is given as

$$\tilde{P} \coloneqq \frac{1}{2}\int_{-\infty}^{-\infty} (j\omega I - A)^{-1} BB'(-j\omega I - A')^{-1}\,\mathrm{d}\omega \quad \text{and}$$
$$\tilde{Q} \coloneqq \frac{1}{2}\int_{-\infty}^{-\infty} (-j\omega I - A')^{-1} C'C(j\omega I - A)^{-1}\,\mathrm{d}\omega \tag{7}$$

Using a linear transformation T for separating the stable (A_s, B_s, C_s, D_s) and antistable (A_{ns}, B_{ns}, C_{ns}, D_{ns}) parts of the system, the generalized controllability $\tilde{P}$ and observability $\tilde{Q}$ gramians defined in Eq. (7) can be constructed:

$$\tilde{P} = T^{-1}\begin{bmatrix} P_s & 0 \\ 0 & P_{\mathrm{ns}} \end{bmatrix}(T^{-1})', \quad \tilde{Q} = T'\begin{bmatrix} Q_s & 0 \\ 0 & Q_{\mathrm{ns}} \end{bmatrix}T \tag{8}$$

where P_s and Q_s are the controllability and observability gramians of (A_s, B_s, C_s), and P_{ns} and Q_{ns} are those of ($-A_{\mathrm{ns}}$, B_{ns}, C_{ns}), which can be computed by solving the Lyapunov equations. The balancing transformation matrix for both the stable and antistable parts then can be calculated as

$$\tilde{V} = UZ\Sigma^{-1/2} \quad \text{and} \quad \tilde{W} = LY\Sigma^{-1/2} \tag{9}$$

where $\tilde{P} = UU^T$ and $\tilde{Q} = LL^T$; and Z, Σ, and Y can be obtained from singular value decomposition (SVD) of $U^TL = Z\Sigma Y^T$. Note that $\tilde{W}^T\tilde{V} = I$. Applying the balancing transformation to the state-space model yields

$$\begin{bmatrix} \dot{x}_b \\ y \end{bmatrix} = \begin{bmatrix} \tilde{W}^TA\tilde{V} & \tilde{W}^TB \\ C\tilde{V} & D \end{bmatrix}\begin{bmatrix} x_b(t) \\ u(t) \end{bmatrix} \tag{10}$$

The state-space model in the new coordinate x_b in Eq. (10) is balanced, and hence, its controllability and observability gramians are equal and diagonal and are sorted in the descending order of the Hankel singular values. By retaining the states corresponding to salient Hankel singular values (e.g., $\sigma_1, \ldots, \sigma_r$) and corresponding columns ($\tilde{W}_r$ and $\tilde{V}_r$) in $\tilde{W}$ and $\tilde{V}$, a ROM without appreciably losing important input/output information can be obtained:

$$\begin{bmatrix} \dot{x}_r \\ y \end{bmatrix} = \begin{bmatrix} A_r(\rho)\ B_r(\rho) \\ C_r(\rho)\ D(\rho) \end{bmatrix}\begin{bmatrix} x_r(t) \\ u(t) \end{bmatrix} \text{ and } \begin{cases} A_r = \tilde{W}_r^TA\tilde{V}_r,\ B_r = \tilde{W}_r^TB \\ B_r = C\tilde{V}_r \end{cases} \tag{11}$$

Note that all unstable modes in X-56A are retained because they contribute to aeroservoelasticity and impose significant impacts to all the input–output channels. Our main consideration of using balanced truncation for unstable systems is that it manipulates stable and unstable modes in the same framework and may offer an opportunity of identifying smooth balancing transformation across the fight envelope and consistent state representation [10].

D. Congruence Transformation and Reduced-Order Model Interpolation

The aforementioned MOR steps are applied to the full-order ASE model at each grid point in the flight envelope, yielding a set of local ROMs $G_{r,i} = [A_{r,i}, B_{r,i}, C_{r,i}, D_{r,i}]$, i.e., Eq. (10), where the subscript i again denotes the ith grid point in the parameter space, and G_r is the reduced system. Given the fact that transformation matrices used in MOR vary along grid points, the physical meaning of the states in each local ROM is not consistent across the flight envelope (i.e., $x_{r,i}$, $\tilde{W}_{r,i}$, and $\tilde{V}_{r,i}$ in the preceding balanced truncation all depend on grid index i). It renders impossible direct interpolation of $G_{r,i}$ to construct ROMs for ASE behavior prediction at arbitrary locations in the parameter space. In other words, states of the reduced system $x_{r,i}$ and of the original system x are related by $\tilde{V}_{r,i}^Tx = x_{r,i}$, and $\tilde{V}_{r,i}$ is grid-dependent. Therefore, $x_{r,i}$ in local ROMs cannot be interpolated directly.

Algorithm 1: Congruence transformation Γ_i at parameters $i(i \neq n_0)$

Input: Right subspace matrices V_i and the reduced system after balanced truncation $G_{r,i} = [A_{r,i}, B_{r,i}, C_{r,i}, D_{r,i}]$
1) Select a reference point n_0 in $i = 1, 2, \text{ and } \ldots, n_s$ and its associated subspace V_{n0}
2) For $i = 1, 2, \ldots, n_s$ and $i \neq n_0$
Compute $M_i = V_i^TV_{n0}$
Compute $M_i = U_i\Sigma_iZ_i^T$ via singular value decomposition (SVD)
Compute $\Gamma_i = U_iZ_i^T$
Compute $A_i^* = \Gamma_i^TA_{r,i}\Gamma_i$, $B_i^* = \Gamma_i^TB_{r,i}$, $C_i^* = C_{r,i}\Gamma_i$, $D_i^* = D_{r,i}$
End for
Output: Transformed system with consistent state representation $G_i^* = [A_i^*, B_i^*, C_i^*, D_i^*]$

To mitigate the issue, one of the most widely used methods is to reproject the individual ROMs onto a common subspace, followed by matrix interpolation, as discussed in [4,8,15]. The common subspace R shared by all local ROMs can be obtained by SVD of the concatenated right projection subspace V_i at grid points (i.e., $RS\Phi^T \approx [V_1, \ldots, V_{\mathrm{ns}}]$, where V_i is the column subspace spanning $\tilde{V}_{r,i}$ in balanced truncation). However, our studies indicate that, because of the broad parameter space and distinctly different dynamic behavior associated with very flexible aircraft, R of a low dimension from SVD cannot effectively capture key bases contained in all V_i [8], leading to poor ROM performance. Therefore, a different approach based on congruence transformation [15] was used. Its principle is to set the right subspace V_{n0} at a grid point n_0 as the reference and then minimize the difference between the subspace V_i at other grid points relative to V_{n0} through the modal assurance criterion (MAC) and changes of basis Γ_i. In other words, a transformation Γ_i at a grid point i is determined to minimize the difference in the Frobenius norm between the $\mathrm{V}_i\Gamma_i$ and V_{n0}:

$$\Gamma_i = \arg\min_{\Gamma_i \in O(r)} \|V_i\Gamma_i - V_{n0}\|_F^2 \tag{12}$$

or equivalently:

$$\Gamma_i = \arg\max_{\Gamma_i \in O(r)} \mathrm{tr}(\Gamma_i^TV_i^TV_{n0}) \tag{13}$$

This is the orthogonal Procurstes optimization problem [16], and a straightforward and analytical solution to computing Γ_i is to take SVD of the relative configuration matrix M_i constructed by the local transformation matrices V_i with respect to the reference matrix V_{n0}. The procedure starts with selecting the right subspace at one parameter as the reference (e.g., V_{n0}) and then iterating on computing the congruence transformation Γ_i at the other parameters relative to the reference [15]. The algorithm is capable of automatically detecting situations where mode crossing and mode veering occurs. Detailed interpretation and comparison of both methods is given in [16]. In this paper, the grid point at the center of the flight parameter space (e.g., 100 KEAS and 40 lb) was selected as the reference point. The congruence transformation is summarized next [15].

Following congruence transformation, the spline interpolation was performed on each individual element in the A_i^*, B_i^*, C_i^*, and D_i^* matrices at grid points to obtain those at nongrid points simply using MATLAB's interp2 function with the option of spline.

IV. Results and Discussion

The LPV state-space models of the X-56A MUTT airframe were used as the example ASE system in our study. They were developed using the generalized mass, stiffness, and aerodynamic matrices obtained by MSC/Nastran** and ZAERO.†† There are 10 control

**Data available online at http://www.mscsoftware.com/product/msc-nastran [retrieved July 2016].

††Data available online at http://www.zonatech.com/ZAERO.htm [retrieved July 2016].

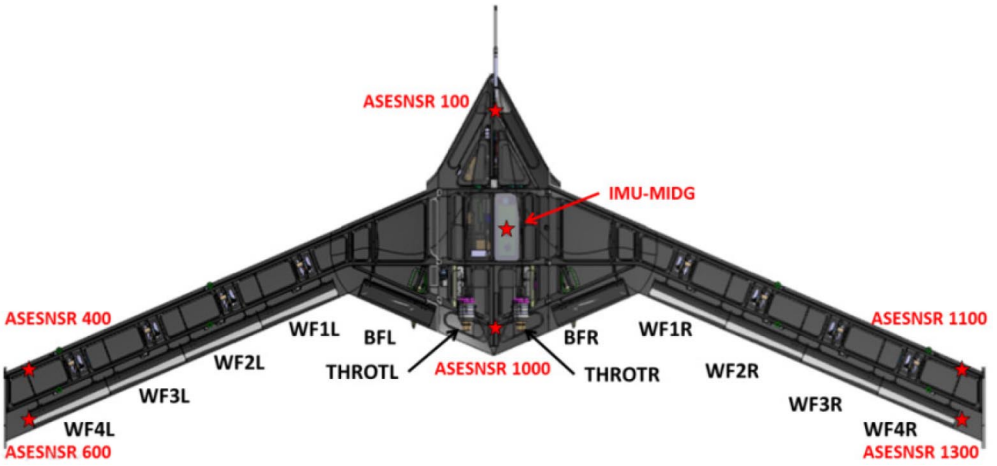

Fig. 3 Sensors and actuators deployment in the X-56A MUTT vehicle.

surfaces on the vehicle, five on each wing, and two throttle controls for engine dynamics, as shown in Fig. 3. The five actuator inputs for control surfaces on the left wing are labeled as BFL, WF1L, WF2L, WF3L, and WF4L, starting from the inner body to the outer wing tip with units of degrees. Likewise, the actuators on the right wing are labeled as BFR, WF1R, WF2R, WF3R, and WF4R based on the same convention. The rigid-body state sensors are located around the center of the vehicle, whereas the ASE accelerometer locations are placed at the front of the vehicle (ASESNSR100), at the rear (ASESNSR1000), at the leading and trailing edge of the left wing (ASESNSR400 and ASESNSR600), and at the leading and trailing edge of the right wing (ASESNSR1100 and ASESNSR1300).

In this paper, the plant model of X-56A MUTT that captures the dynamics and ASE behavior associated with the pitch axis was used. A set of 357 (21×17) models were generated at $M = 0.16$ on grid points of a 2-D parameter space across the flight envelope. The two parameters are knots equivalent airspeed (KEAS), which ranges from 50 to 150 KEAS in 5 KEAS increments, and fuel weight, which ranges from 0 to 80 lb in 5 lb increments. The model at each grid point has 192 states, including 56 states corresponding to the second-order sensors (28 sensors in total), 12 rigid body states, 14 elastic structural modes and 14 derivatives (modal velocity), 60 aerodynamic lag states, and 36 states for the third-order actuators (10 control surfaces and two engine throttles). According to the $V-g$ and $V-f$ plots of the X-56A baseline model at $M = 0.16$ [17], the normalized flutter frequencies for symmetric body freedom flutter (SBFF), symmetric wing bending torsion flutter (SWBTF), and antisymmetric wing bending torsion flutter (AWBTF) modes are, respectively, at 1, 3.68, and 3.912 (all the flutter frequencies are normalized by the one for SBFF due to ITAR requirement). The target normalized frequency range ω for X-56A model reduction is determined to be $0.01 < \omega < 5.37$ to ensure full coverage of the instability of interest and system response.

Instead of using raw inputs and outputs, composite inputs and outputs relevant to pitch dynamics constructed by the raw ones were included in the model to facilitate controller synthesis. Specifically for input channels, the control surfaces were symmetrically combined to form new inputs to the pitch plant model, e.g., BFL and BFR coupled as $(\mathrm{BFL} + \mathrm{BFR})/2$, and the same is applied to all other inputs. Similarly in addition to qb, the pitch rate of the aircraft, three composite outputs (i.e., ASE 1, ASE 2, and ASE 3) were constructed using raw sensor outputs, specifically, ASE1 = (ASESNSR400+ASESNSR1100 −ASESNSR600−ASESNSR1300)/4; ASE2 = (ASESNSR400 +ASESNSR1100+ASESNSR600+ASESNSR1300)/4; and ASE3 = (0.28× ASESNSR1000−0.72×ASESNSR100). All the labeling is given in Fig. 3.

The MOR framework described in Sec. III was then applied to the X-56A MUTT ASE model. Truncation and residualization was used to eliminate the states associated with sensors, actuators, aerodynamic states, rigid-body states, and elastic states. The aforementioned GA was employed to select states of aerodynamic lags and elastic structural modes and modal velocities for reduction due to their largest contribution to the total state numbers and the difficulty of manual selection. It was then followed by transformation-based MOR (balanced truncation for unstable systems). Changes of basis based on congruence transformation were then applied to ROMs to achieve the most state consistence among local ROMs, rendering them ready for interpolation. The matrix entries of ROMs were then interpolated using the spline interpolation, yielding LPV ROM at any location in the 2-D flight parameter space. The following studies include verifying the MOR methodology by comparing ROMs against the full X-56A MUTT model, examining consistence in state presentation, and evaluating ROM interpolation. For sake of brevity, only four input–output channels are shown, viz., from inner body $(\mathrm{BFL} + \mathrm{BFR})/2$ to pitch rate (qb) and ASE1, and from wing tip $(\mathrm{WF4}R + \mathrm{WF4}L)/2$ to pitch rate (pb) and ASE1. The center grid point in the flight envelope (100 KEAS and 40 lb) serves as the benchmark case.

A. Sequential Model Order Reduction

The sequential MOR including sensor reduction, actuator reduction, aerodynamic lag reduction, rigid-body reduction, elastic state reduction, and balanced truncation was performed in the benchmark case.

1) Sensor reduction: Given independent nature of the sensors states in the full-order model, we first truncated 42 states in the 56 sensor states that have no contribution to pitch-axis observation. Then, the remaining 14 states associated with the first- and second-order sensor dynamics in study were fully residualized to match the dc gain of the full model, leading to a ROM with 136 states.

2) Actuator reduction: The X-56A MUTT model includes 10 surface controls and two engine controls, and each is described by third-order dynamics. Six states corresponding to engine throttle controls that are not the object of our ASE study were truncated. Next the third-order states of the remaining 10 surface control actuators in the study (i.e., BFL, WF1L–WF4L and BFR, WF1R–WF4R) were residualized, yielding a ROM of 120 states with the second-order approximation of actuator dynamics.

3) Aerodynamic lag reduction: The X-56A MUTT model includes 60 aerodynamic lag states in the full model. In contrast to the trial-and-error approach in previous efforts, the GA-guided truncation and residualization was used to reduce 36 aerodynamic states, yielding a ROM of 84 states. The GA-guided approach will be compared against the manual selection approach, whereas in the latter, the first 24 leading aerodynamic lag states were retained.

4) Rigid-body reduction: The X-56A MUTT model has 12 rigid body states in the full-order model, which are x, y, ψ, h, ϕ, θ, u, β, α, p, q, and r. Several comparative studies were carried out in which various combinations of the rigid-body states were examined to

Table 1 Sequential MOR and resulting model sizes

Reduction	Original	Sensor	Actuator	Aerodynamic	Rigid body	Elastic	Balanced truncation
Model size	192	136	120	84	76	58	16

determine the best set that has negligible impact to system dynamics, resulting in a ROM with 76 states with consistent performance across the entire flight envelope.

5) Elastic state reduction: The X-56A MUTT model has 14 coupled elastic modes, corresponding to 28 states. The first 14 states were used to describe the modal displacements, whereas the rest were used for the modal velocity. The GA-guided approach suggested keeping five states each in modal displacement and modal velocity in the ROM, that is, 18 states in total were residualized, yielding a ROM with 58 states. The GA-guided approach will be compared against the manual selection approach, and in the latter, the first five leading states in the modal displacement and velocity (10 in total) were kept.

6) Balanced truncation for unstable systems: It was used to transform the 58-state ROMs into a balanced controllable and observable form using the stable/antistable state separation and generalized balancing transformation. The states in the model were sorted according to the significance of their corresponding Hankel singular values. Therefore, the states with the least controllability and observability were removed to construct the minimal realization of the model capable of capturing the dynamics between all input–output pairs. In this study, 27 states with smaller Hankel singular values were truncated, yielding a ROM with 16 states.

The sequential MOR and resulting model sizes are summarized in Table 1. Figures 4 and 5 show the comparison of the magnitude and phase in the frequency domain between the original full-order X-56A and ROM for the benchmark case (100 KEAS 40 lb) during the sequential MOR. It demonstrates that ROM accurately matches the original model for all the selected input–output channels within the desired frequency range, whereas the number of states is reduced by 12×.

The results of truncation and residualization based on GA and manual selection are compared in Fig. 4. Given a budget of 24 states in aerodynamic lags and 10 elastic states, GA was used to automatically determine the most important ones to preserve the dynamics of the original system, whereas in manual selection, the elastic states correspond to the first five modal displacements and velocities, and the first 24 aerodynamic states were retained. The GA-ROM outperforms the manual ROM dramatically in all input–output channels, in particular the input channel $(\mathrm{BFL}+\mathrm{BFR})/2$, confirming the performance of GA in identifying important states in the system. Figure 5 illustrates the comparison of the final ROM obtained by balanced truncation against the original model. The ROM of 58 states following elastic reduction was transformed into the balanced form, and 42 states with smallest Hankel values were then truncated, resulting in a final ROM with only 16 states. It can be

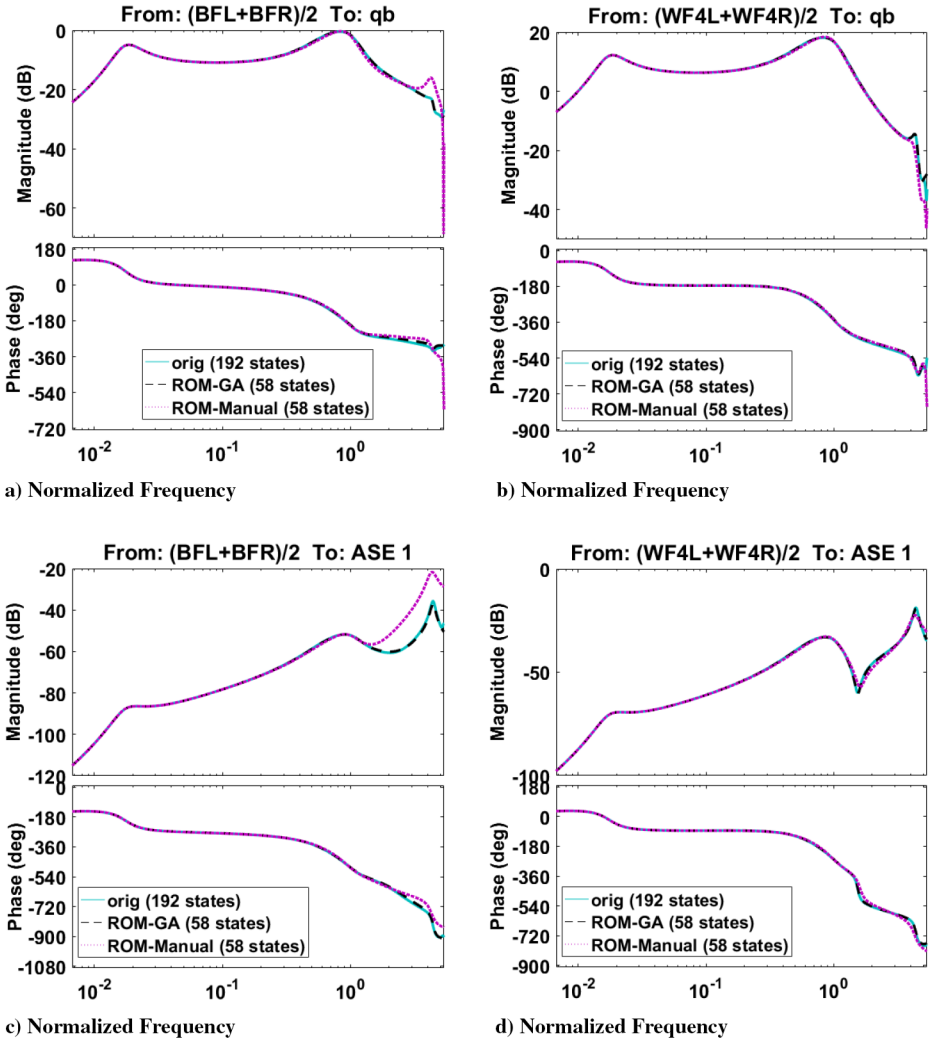

Fig. 4 Magnitude and phase comparison between the original, full X-56A model (192 states) and the ROM after elastic state reduction.

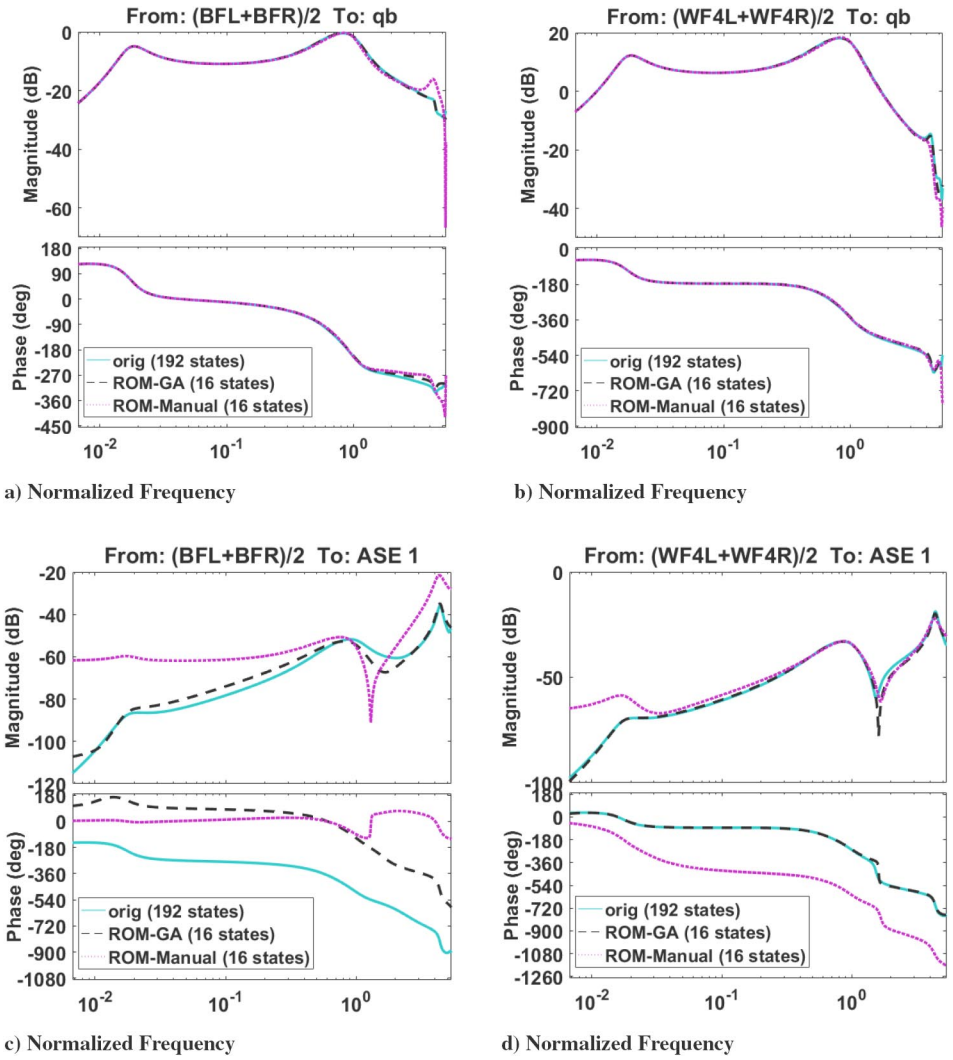

Fig. 5 Comparison in magnitude and phase between the original, full X-56A model (192 states) and the ROM after unstable balanced truncation.

clearly been seen that salient performance by the GA was carried over to the downstream analysis. The GA-guided ROM resolves dynamics among all channels very well, whereas the manually selected ROM failed to capture the system response at all frequency regime in the ASE1 channel as well as high-frequency regimes in qb channel.

B. Consistent State Representation and Reduced-Order Model Interpolation

Consistent state representation based on congruence transformation and ROM interpolation were then undertaken to achieve LPV ASE ROMs, as described in Sec. III. Figure 6 shows the pole migration for both the original full (192 state) and reduced (16 state) systems. Again, the real and imagery axes are normalized by the flutter frequency of SBFF. In Figs. 6a and 6b, the fuel weight is fixed at 40 lb, and the speed increases from 50 to 150 KEAS. The original model and ROM at the grid points with a resolution of 5 KEAS are directly available, whereas those between the grid points were obtained by interpolating the models at the grid points (at a resolution of 2 KEAS). In Figs. 6c and 6d, the speed is kept constant at 100 KEAS, and poles are shown for fuel weights between 0 and 80 lb at a resolution of 2 lb. It is clear that the poles translate smoothly from one parameter value to another, thus confirming the state consistence at grid point achieved by congruence transformation. Comparison of the left column against the right column also reveals that the unstable modes of the original system in target frequency range are completely preserved, and the ROM can be used for controller synthesis. It is noted that the interesting phenomenon of pole conversion (i.e., real poles change into conjugate pairs or vice versa) from a parameter to another also occurs in the original model and ROM of X-56A MUTT. In the ROM, between 106 and 108 KEAS, the number of real poles decreases from 2 to 0, whereas between 70 and 72 lb, the number of real poles increases from 2 to 4. In all cases, the consistent state representation is maintained well, as indicated by continuous pole migration. This further substantiates that our MOR methodology is capable of tackling the issue of pole conversion, which otherwise may not be addressed by the modal matching method [7].

Figure 7 illustrates the magnitude of Bode diagram as a function of airspeed (KEAS) at a fixed fuel weight of 40 lb. The left, middle, and right columns, respectively, are the results for the interpolated original model (192 state) and the interpolated ROM (16 state) without and with congruence transformation. Figure 8 displays similar results as a function of fuel weights (pounds) while airspeed is kept constant at 100 KEAS. The interpolation was carried out on a grid of 5 KEAS $\times$ 5 lb with a resolution of 1 KEAS $\times$ 1 lb for enhanced visualization. The results produced by the interpolated original model (i.e., Figs. 7a, 7d and Figs. 8a, 8d are used as the baseline). Comparing the second column (i.e., Figs. 7b, 7e and Figs. 8b, 8e) and the third column (i.e., Figs. 7c, 7f and Figs. 8c, 8f) against the baseline results reveals the effects and necessity of using congruence transformation before ROM interpolation. The interpolated ROM based on consistent state representation (the third column) resembles the dynamics of the original model (the first column). The salient performance is most evident at around 100 KEAS in Fig. 7 and 80 lb in Fig. 8, where the interpolation is even able to capture the peak response. The ROM without state consistence (the second column) exhibits significant discontinuities and physically meaningless dynamics, resulting in poor interpolation

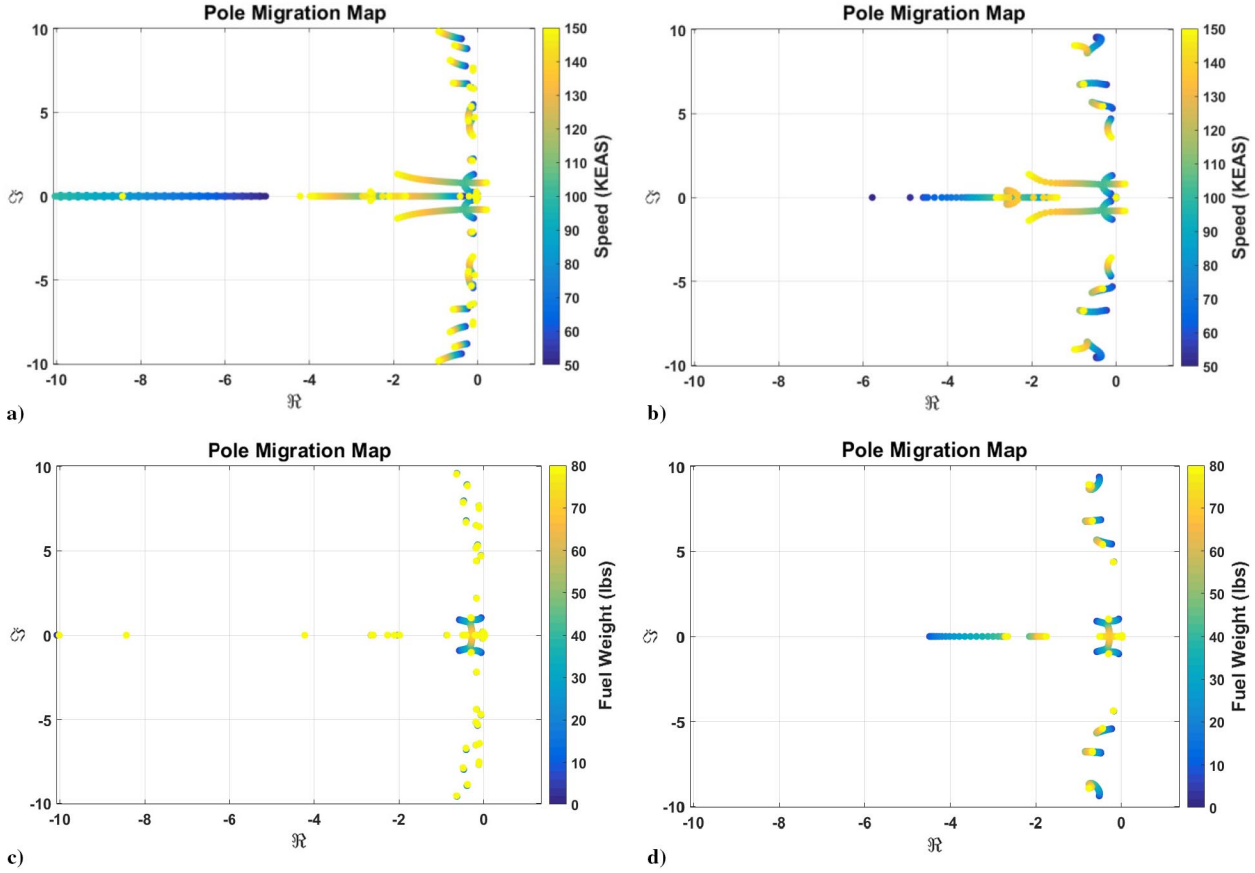

Fig. 6 Pole migration for original model (left) and ROM (right): a–b) fuel weight at 40 lb, and c–d) speed at 100 KEAS.

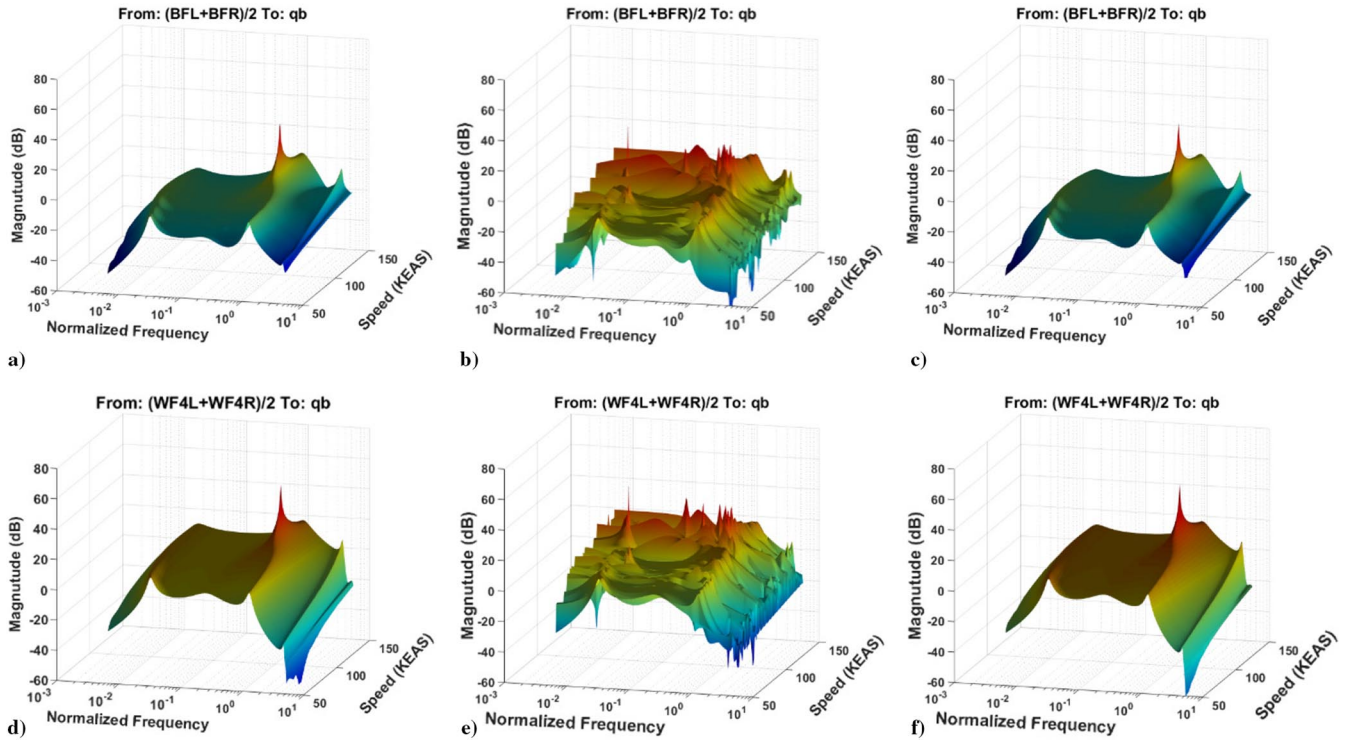

Fig. 7 Bode diagram as a function of speed at a fixed fuel weight of 40 lb.

performance. A slight discrepancy between interpolated ROM with congruence transformation and the baseline results at the high-frequency regime is also observed in both figures, which is expected because it is also present in the ROM on the grid (see Figs. 4 and 5) due to large reduction in the state number. Such behavior will obviously translate to the interpolated results.

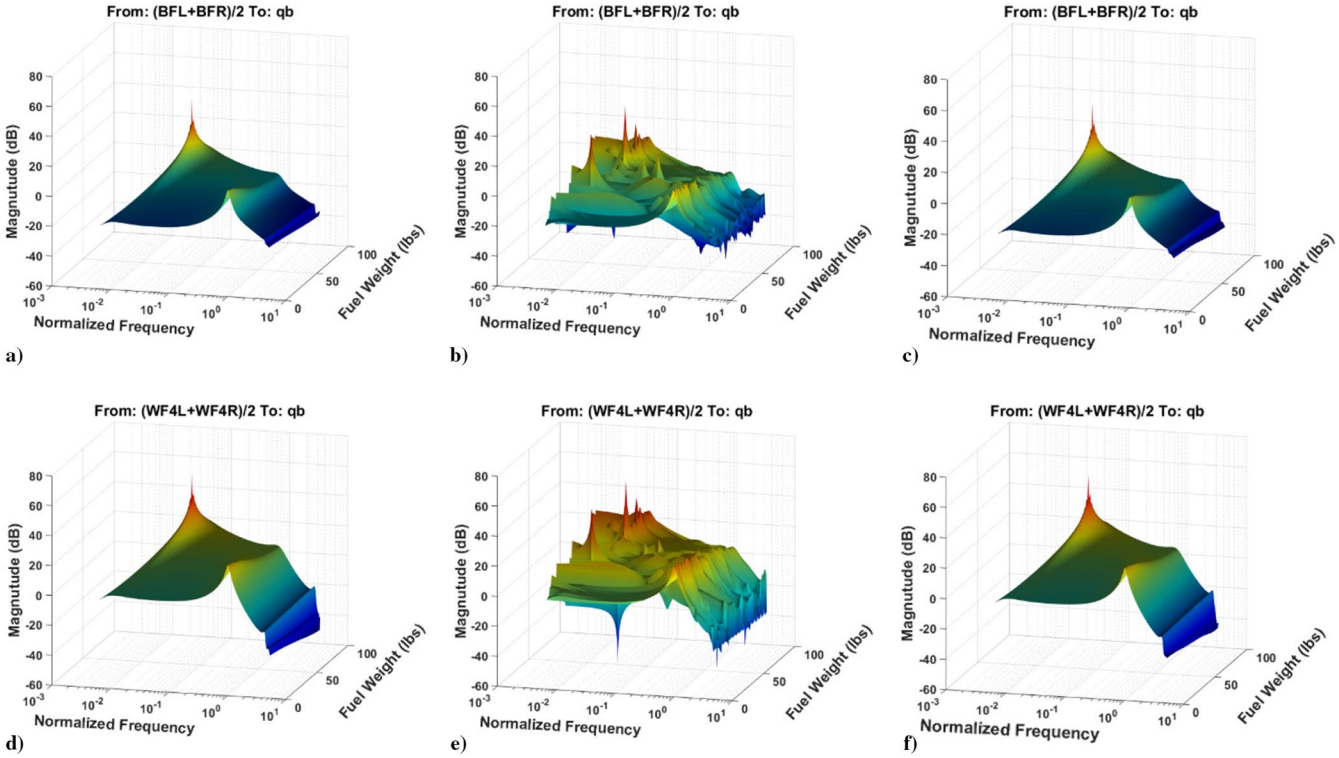

Fig. 8 Bode diagram as a function of fuel weight at a fixed speed of 100 KEAS.

V. Conclusions

An automated model order reduction (MOR) framework based on the genetic algorithm (GA) and congruence transformation has been presented for linear parameter-varying (LPV) aeroservoelastic (ASE) systems of flexible aircraft. The MOR includes two key steps (i.e., local model reduction and model interpolation). In the former, the full-scale ASE model is first reduced through truncation and residualization of unimportant states in the system under various categories, including sensors, actuators, rigid body, aerodynamic lag, and elastic states. A process relying on GA and globally meaningful objective function was developed to intelligently determine the optimal states across the broader 2-D flight parameter space that could be removed while imposing minimal impact on the system response within the target frequency range. The GA-guided truncation and residualization maintains the state consistence among the local ROMs. The resulting local models then undergo balanced truncation for unstable system based on the generalized gramians to further eliminate states with minimal contribution to the system dynamics along input/output channels. It is followed by congruence transformation for weak fulfillment of state consistency across the entire flight parameter space. Finally, all the local ROMs with consistent state representation are amenable to spline interpolation of model matrices for constructing ASE ROMs at any location in the parameter space.

The MOR methodology was verified using NASA's X-56A MUTT model. The present investigations show that the original pitch plant model of 192 states could be reduced down to 58 states by the aforementioned GA-guided truncation and residualization and further 16 states by balanced truncation for unstable systems. The resulting ROM with 12× reduction in the number of states is able to not only match dynamics of the original ASE system with a high degree of accuracy but also outperform the ROM involving manual selection of states for reduction, clearly confirming the utility of the present GA-guided method. The feasibility of consistent state representation achieved by congruence transformation was also inspected by the pole migration and Bode diagram of the interpolated ROMs and their comparison against the original model. The interpolated ROMs exhibit smooth pole transition and continuously varying gains along different fuel weights and air speed and hence are applicable to constructing ASE ROMs at any location in the parameter space.

The reported research develops LPV ROMs with consistent state representation in broad 2-D flight parameter space for unstable ASE systems with pole conversion and enables robust and efficient ASE controller synthesis for aircraft, novel vehicle design for flutter suppression and gust load alleviation, and notable reduction in development time and cost.

Acknowledgment

This research is sponsored by NASA Armstrong Flight Research Center under contract NNX15CD03C.

References

[1] Antoulas, A. C., "An Overview of Approximation Methods for Large-Scale Dynamical Systems," *Annual Reviews in Control*, Vol. 29, No. 2, 2005, pp. 181–190. doi:10.1016/j.arcontrol.2005.08.002

[2] Hjartarson, A., Seiler, P. J., and Balas, G. J., "LPV Aeroservoelastic Control Using the LPVTools Toolbox," *AIAA Atmospheric Flight Mechanics (AFM) Conference*, AIAA Paper 2013-4742, 2013.

[3] Moreno, C. P., Seiler, P. J., and Balas, G. J., "Model Reduction for Aeroservoelastic Systems," *Journal of Aircraft*, Vol. 51, No. 1, 2014, pp. 280–290. doi:10.2514/1.C032341

[4] Panzer, H., Mohring, J., Eid, R., and Lohmann, B., "Parametric Model Order Reduction by Matrix Interpolation," *at-Automatisierungstechnik Methoden und Anwendungen der Steuerungs-, Regelungs- und Informationstechnik*, Vol. 58, No. 8, 2010, pp. 475–484.

[5] Poussot-Vassal, C., and Roos, C., "Flexible Aircraft Reduced-Order LPV Model Generation from a Set of Large-Scale LTI Models," *Proceedings of the American Control Conference (ACC)*, IEEE Publ., Piscataway, NJ, 2011, pp. 745–750.

[6] Poussot-Vassal, C., and Demourant, F., "Dynamical Medium (Large)-Scale Model Reduction and Interpolation with Application to Aircraft Systems," *Aerospace Lab.*, No. 4, 2012, pp. 1–0.

[7] Theis, J., Takarics, B., Pfifer, H., Balas, G., and Werner, H., "Modal Matching for LPV Model Reduction of Aeroservoelastic Vehicles," *AIAA Atmospheric Flight Mechanics Conference*, AIAA Paper 2015-1686, 2015.

[8] Wang, Y., Song, H., Pant, K., Brenner, M. J., and Suh, P. M., "Model Order Reduction of Aeroservoelastic Model of Flexible Aircraft," *57th*

AIAA/ASCE/AHS/ASC Structures, Structural Dynamics, and Materials Conference, AIAA Paper 2016-1222, 2016.

[9] Schmidt, D. K., "Stability Augmentation and Active Flutter Suppression of a Flexible Flying-Wing Drone," *Journal of Guidance, Control, and Dynamics*, Vol. 39, No. 3, 2016, pp. 409–422.

[10] Moreno, C., Seiler, P., and Balas, G. J., "Linear Parameter Varying Model Reduction for Aeroservoelastic Systems," *AIAA Atmospheric Flight Mechanics Conference*, AIAA Paper 2012-4859, Aug. 2012.

[11] Mitchell, M., *An Introduction to Genetic Algorithms*, A Bradford Book The MIT Press, Cambridge, 1996, pp. 87–130.

[12] Beasley, D., Bull, D. R., and Martin, R. R., "An Overview of Genetic Algorithms: Part 2, Research Topics," *University Computing*, Vol. 15, No. 4, 1993, pp. 170–181.

[13] Beasley, D., Martin, R., and Bull, D., "An Overview of Genetic Algorithms: Part 1, Fundamentals," *University Computing*, Vol. 15, No. 2, 1993, pp. 58–69.

[14] Zhou, K., Salomon, G., and Wu, E., "Balanced Realization and Model Reduction for Unstable Systems," *International Journal of Robust and Nonlinear Control*, Vol. 9, No. 3, 1999, pp. 183–198. doi:10.1002/(ISSN)1099-1239

[15] Amsallem, D., and Farhat, C., "An Online Method for Interpolating Linear Parametric Reduced-Order Models," *SIAM Journal on Scientific Computing*, Vol. 33, No. 5, 2011, pp. 2169–2198. doi:10.1137/100813051

[16] Geuss, M., Panzer, H., and Lohmann, B., "On Parametric Model Order Reduction by Matrix Interpolation," *Proceedings of the 2013 European Control Conference (ECC)*, Inst. of Electrical and Electronics Engineers, New York, 2013, pp. 3433–3438.

[17] Pak, C.-G., and Truong, S., "Creating a Test Validated Structural Dynamic Finite Element Model of the X-56A Aircraft," *15th AIAA/ISSMO Multidisciplinary Analysis and Optimization Conference*, AIAA Paper 2014-3157, 2014.